

The Explorative Analysis to Revise Fear Network Model for Panic Disorder

Functional Connectome Statistics

Chien-Han Lai, MD, PhD and Yu-Te Wu, PhD

Abstract: Functional connectome analysis in panic disorder (PDO) is a relatively new field for research. We tried to investigate the functional connectome alterations in PDO to re-examine the precision and role of fear network model for the pathophysiology of PDO.

We enrolled 53 PDO patients and 54 controls with imaging data in this study. After preprocessing, we calculated the connectivity matrix of functional connectivity in whole brain for each subject. Then network-based statistics (The University of Melbourne and Melbourne Health, Australia) of connectome was used to perform group comparisons between patients and controls. The correlation between network measures of significant subnetwork and illness duration or severity of PDO was also performed.

Within the 6 network models, only 1 network survived after multiple corrections. We found decreased functional connectivity in the edges between the following nodes: the left parahippocampal gyrus, bilateral precentral gyri, bilateral middle cingulate gyri, bilateral supramarginal gyri, bilateral calcarine fissures, and right lingual gyrus. The central hubs were the left parahippocampal gyrus and left precentral gyrus. The importance of limbic areas and connection with sensory and motor

regions might shed light on the revision of fear network model for the pathophysiology of PDO.

(*Medicine* 95(18):e3597)

Abbreviations: CAL.L and CAL.R = left and right calcarine fissure, DCG.L and DCG.R = left and right middle cingulate gyrus, HARS = Hamilton Rating Scales for Anxiety, HDRS = Hamilton Rating Scales for Depression, LING.R = right lingual gyrus, NBS = network-based statistics, PDO = panic disorder, PDSS = panic disorder severity scale, PHG.L = left parahippocampal gyrus, PreCG.L = left precentral gyrus, Rs-FMRI = resting-state functional magnetic resonance imaging, SMG.L and SMG.R = left and right supramarginal gyrus.

INTRODUCTION

Panic disorder (PDO) consists of somatic symptoms, such as chest tightness, dizziness, palpitations, abdominal discomforts, feel like dying, and feel like losing control. It is easily comorbid with other psychiatric illnesses and causes significant impairments in functions.^{1,2} The pathophysiology model of PDO originated from “fear network” hypothesis, which includes limbic and sensory-related regions, such as frontal cortex, insula, amygdala, hippocampus, and sensory cortex. The hyperactive limbic response associated with oversensitive sensory function will reduce the inhibitory action from frontal cortex, which causes the panic attacks.³ The dysfunctional coordination of “upstream” (cortical) and “downstream” (brainstem) sensory information leads to heightened amygdala activity with subsequent behavioral, autonomic, and neuroendocrine activation. The sensory-related regions are connected with limbic areas to manage the oversensitivity to unknown fear. An inadequate control of fear responses will provoke panic attacks. However, the latest revised model of “fear network” suggested the potential extension of the model to several regions beyond the original neuroanatomical model, such as anterior cingulate cortex and insula.⁴

The limbic regions in the fear network model for PDO includes parahippocampal gyrus (PHG), cingulate cortex, and amygdala.³ Previous structural reports of PDO revealed the gray matter reductions in the left PHG (PHG.L)⁵ and the right PHG (PHG.R).^{6,7} The functional studies also demonstrated altered binding in the benzodiazepine receptors of PHG, which was also negatively associated with panic severity.⁸ Hyperactivity of PHG and cingulate cortex was also noted in the provoking model for PDO.⁹ Therefore, the limbic system, especially the PHG, played a crucial role for PDO.

The PDO-related sensory region¹⁰ usually involved the functions of visuospatial transformation, attention, perception, recognition memory, and the processing of interoceptive sensory information.¹¹⁻¹³ Visual cortex also processes visual

Editor: Numan Konuk.

Received: February 12, 2016; revised: April 5, 2016; accepted: April 12, 2016.

From the Department of Psychiatry (C-HL), Cheng Hsin General Hospital, Taipei City; Department of Biomedical Imaging and Radiological Sciences (C-HL, Y-TW); Institute of Biophotonics (C-HL, Y-TW); and Brain Research Center (Y-TW), National Yang-Ming University, Taipei, Taiwan, ROC.

Correspondence: Chien-Han Lai, Department of Psychiatry, Cheng Hsin General Hospital, No. 45, Cheng Hsin St, Pai-Tou District, Taipei City, Taiwan, ROC (e-mail: stephenlai99@gmail.com).

C-HL collected data, researched data, and wrote manuscript. Y-TW reviewed and edited the manuscript.

Disclosures: All individuals included as authors have contributed substantially to the scientific process leading up to the writing of the paper. In addition, the authors have made a substantial contribution to drafting or critical revision of the manuscript for important intellectual content.

The study was supported by Buddhist Tzu-Chi General Hospital, Taipei Branch hospital project TCRD-TPE-99-02 and grant from the Cheng Hsin General Hospital and National Yang Ming University cooperative project 105F003C03.

This study was also funded by Taipei Tzu-Chi General Hospital project TCRD-TPE-99-02 and grant from the Cheng Hsin General Hospital and National Yang Ming University cooperative project 104F003C03.

All procedures performed in studies involving human participants were in accordance with the ethical standards of the institutional and/or national research committee and with the 1964 Helsinki declaration and its later amendments or comparable ethical standards.

Informed consent was obtained from all individual participants included in the study.

The authors report no conflicts of interest.

Copyright © 2016 Wolters Kluwer Health, Inc. All rights reserved.

This is an open access article distributed under the Creative Commons Attribution-NonCommercial-NoDerivatives License 4.0, where it is permissible to download, share and reproduce the work in any medium, provided it is properly cited. The work cannot be changed in any way or used commercially.

ISSN: 0025-7974

DOI: 10.1097/MD.0000000000003597

imagery and regulates autonomic function, which is also related to panic attacks.¹⁴ Panic-like responses, which are induced by shock-related fear with impaired consolidation of extinction of fear changes, are also associated with altered activities in bilateral lingual gyrus.¹⁵ The results are also in line with abnormal spatial-related attention and impaired connection between amygdala and visual area in PD.¹⁶

Resting-state functional magnetic resonance imaging (Rs-FMRI) is an important technique for acquisition of baseline brain activity, which can be used to assess the functional connectivity. The whole-brain functional connectome has been an emerging area for the investigation of pathophysiology for mental illnesses. Recently, a new method, network-based statistics (NBS), has been applied in the field of connectome analysis. It uses the graph theory concept to derive the large-scale brain connectivity with the control of family-wise error due to mass-univariate testing for each connection of the functional or structural connectome.¹⁷ It has been applied in several psychiatric illnesses, such as functional connectome in schizophrenia¹⁷ and structural connectome in depression.^{18,19}

In this study, we investigated the functional connectome of first-onset, medicine-naïve patients with PDO. We used the NBS method to conduct the connectome analysis. According to the above literature, we hypothesized that functional connectome would be compatible with latest revised model of PDO,⁴ which mostly included the potential extension of limbic and sensory regions. We also hoped to find the central hubs for the functional connectome within the “fear network.”

METHODS

Participants

The PDO group was enrolled according to the following criteria: first-onset patients with a pure PDO diagnosis (The Diagnostic and Statistical Manual of Mental Disorders Fourth Edition criteria); Clinician Global Impression of Severity >4, Quick Inventory for Depressive Symptoms-Self Rating 16-item version (QIDS-SR16) <9,²⁰ Hamilton Rating Scales for Depression (HDRS) score <7²¹ (to avoid the comorbidity of depression), Hamilton Rating Scales for Anxiety (HARS) score >22,²² Panic Disorder Symptom Severity Scale (PDSS) >15,²³ and the other criteria listed in our previous study.²⁴ The healthy controls had no psychiatric illnesses (according to brief psychiatric rating scale 18-item version, all items must be “not present”) or significant medical illnesses (according to medical records). All patients and healthy subjects signed the informed consent that was approved by the 3 Institutional Review Boards at Taipei Tzu Chi Hospital, Cheng Hsin General Hospital, and National Yang-Ming University, according to the institute where they were recruited. None of the participants received psychotropic treatment while on Rs-FMRI scanning. Edinburgh Inventory of Handedness was used to assess the handedness.²⁵ Eighty-nine patients were screened and 36 patients were excluded due to noncompatibility with the selection criteria. Fifty-three patients and 54 controls were selected. The sample of participants had some overlaps of our previous studies, which was around 50% overlap.^{26,27}

Rs-FMRI Data Acquisition

Echo planar imaging (EPI) sequence (repetition time = 2000 ms, echo time = 40 ms, field of view = 24 cm; 5 mm thickness; 150 time points, voxel dimension: 64 × 64 × 20) was acquired at baseline visit (3T Siemens scanner housed at

magnetic resonance center of National Yang Ming University) in patients and controls. For the detailed information of pulse sequence and other procedures for Rs-FMRI scanning, please refer to our previous study.²⁴

Rs-FMRI Data Preprocessing

The EPI data were first preprocessed by Data Processing Assistant and Resting-State FMRI (DPARSF, version 2.2; Beijing Normal University, China),²⁸ which included the removal of first 10 time points, slice timing, realignment, normalization, resampling, smoothing by Full Width at Half Maximum (FWHM) 4 × 4 × 4 kernel, to detrend and filter data with residual signals within 0.01 to 0.08 Hz to discard physiological noise and drift.²⁴ No subject was excluded because no excessive motions were observed. The filtered Rs-FMRI data were registered (nonlinear elastic registration) to study-specific template. The effects of “micromovements” and the nuisance correlation caused by head motion were removed by checking covariates in nuisance regressors in DPARSF.^{29,30} Several spurious covariates were removed except global signals.^{31,32} The individual-level covariates of motion and group-level covariates of motion were adjusted using Friston-24 parameter model and frame-wise displacement motion regression model, respectively.^{24,33}

Connectivity Matrix Measures

We used the GRaph thEoretical Network Analysis (GRETNA) toolbox (<https://www.nitrc.org/projects/gretna>) to calculate the connectivity matrix for the preprocessed Rs-FMRI data of each subject. GRETNA toolbox has been designed for the graph-theoretical network analysis of Rs-FMRI data. It is a suite of MATLAB functions and some MATLAB-based Interface to perform the process of conventional functional preprocessing, and also to calculate most frequently used connectivity matrix.

NBS Analysis

The NBS is used for multifactorial designs stemming from the functional connectivity in this study. It was used to identify significant differences between patients and controls for pair-wise associations. It incorporated graph model to identify the pair-wise association, such as the connection or link, between different pairs of nodes.¹⁷

The processing steps were as follows:

- (1) The design matrix was set at first to define the group and number for subjects of patients and controls. Then, we put the connectivity matrix file for each subject as the input data. From the probability point, the $N(N-1)/2$ unique pair-wise associations would be possible for a $N \times N$ connectivity matrix. For each pair-wise association, the test statistic of interest was calculated independently using the values stored in each subject's connectivity matrix, such as Fisher *r*-to-*z* transform for a correlation-based measure of association to ensure normality.
- (2) The AAL-90 nodes and labels were used to define and locate the significant nodes within the significant subnetwork in a graph model. A nonparametric test was used for a breadth first search. *N* was the number of nodes. This was repeated for *M* permutations to estimate the null distribution. The random permutations were generated independently and the group to which each subject belonged was randomly exchanged for each permutation. The number or size of links the potential nodes was decided according to the threshold (corrected $P < 0.05$). Permutation testing was used to

ascribe a *P* value controlled for the FWE to each connected component based on its size.

- (3) The test statistic of interest was recalculated for each permutation, which can detect the potential connection of suprathreshold links and demonstrate the topological connection. An empirical estimate of the null distribution of maximal component size was also obtained by the above permutation.
- (4) Finally, the *P* value (0.05) of an observed component of size *k* was estimated by finding the total number of permutations to identify maximal component size.

The importance of NBS is to translate and apply the graph model. The approach can be generalized to multifactorial designs and compute the set of all connected components in a graph model. It was comprehensive and appropriate for our goal to estimate the significant subnetwork from the viewpoint of whole brain.

Statistical Analysis

The chi-square test was used to estimate sex difference. The differences in the demographic data and clinical severity, such as age, educational years, HARS scores, and PDSS scores, between patients and controls, were estimated by the Mann–Whitney *U* test. The association between functional connectivity and clinical variables (eg, panic severity, anxiety severity, illness duration) with demographic covariates (age, sex) was also evaluated (statistical threshold: corrected *P* < 0.05). The correlation assessment was only used for significant network edges identified by the NBS method.

RESULTS

Demographic Data

There were no significant differences in age, sex, handedness, educational years, and HDRS scores between patients and controls. The duration of illness in patient group was 5.35 ± 2.37 months. On the contrary, there was significant difference in HARS scores between patient and controls. In addition, the PDSS scores of patients were 21.43 ± 1.91 (Table 1).

NBS Results: Alterations in Functional Connectome of PDO

In the NBS analysis, the patients with PDO had significantly lower functional connectivity strength. There were 6

connectivity networks observed with just 1 functional connectivity network survived multiple comparison (corrected *P* = 0.037). The number of nodes were 9 and the number of edges were 8 (Table 2). The nodes included PHG.L, left precentral gyrus (PreCG.L), left middle cingulated gyrus (DCG.L) and right middle cingulated gyrus (DCG.R), left supramarginal gyrus (SMG.L) and right supramarginal gyrus (SMG.R), left calcarine fissure (CAL.L) and right calcarine fissure (CAL.R), and right lingual gyrus (LING.R). The edges revealed important role of 2 central hubs—the PHG.L and PreCG.L. Within the 2 major hubs, the PHG.L seemed to have a bottom-up mechanism towards the PreCG.L (Table 2, Figure 1). However, the correlation analysis between PDSS or HARS scores and functional connectivity strength revealed no significant results (uncorrected *P* = 0.12).

DISCUSSION

In this study, we proved the importance of fear network model in the pathophysiology of PDO. Our findings suggested that dominant role of limbic system (PHG.L) might be related to the dysregulation of brain homeostasis in PDO. The 2 central hubs (the command centers of the network), the PHG.L and PreCG.L, in current study, also supported our hypothesis to find the connectome compatible with revised fear network model for PDO.³⁴ The alterations in functional connectome consisted of 9 nodes (the network spots) and 8 edges (the links between network spots), and suggested that patients with PDO probably had significant functional alterations in limbic (PHG.L and DCG), sensory (CAL, LING, and SMG), and motor (PreCG) regions. The alteration in DCG was compatible with the additional region in the revised model of fear network proposed by Dresler et al.³⁴ It was also in line with the “top-down” dysregulation in the fear network model. The findings of PreCG.L were not expected by our original hypothesis based on the “fear network model.” The study revealed the possible revision of original “fear network model” for the origin of panic symptoms. The findings of the current study suggested that we should reconsider the role of motor region, such as PreCG.L, in the fear network model. The current analysis of functional connectome strengthened the possible background of PreCG for the panic attacks-related motor symptoms, such as fright, fear to lose control, and escape behavior. The findings of PHG were consistent with the fear network model and the crucial hub role also strengthened the important role of PHG. In addition, other limbic nodes, such as DCG.L and DCG.R, also support the crucial role of limbic regions in the functional

TABLE 1. Demographic data of participating patients and controls

| | Patients (n = 53) | Controls (n = 54) | Sig <i>P</i> (2-tailed), <i>Z</i> , <i>df</i> = 63 |
|--|-------------------|-------------------|--|
| Age, mean (SD), years old | 43.28 (10.11) | 40.38 (10.51) | 0.101, −1.64 |
| Sex (number) | F (28), M (25) | F (29), M (25) | 0.518 |
| Duration of illness, mean (SD), months | 5.35 (2.37) | 0 (0) | N/A |
| Educational years, mean (SD) | 15.94 (1.08) | 16.14 (0.76) | 0.232, −1.196 |
| Handedness | >R (52), L (1) | R (52), L (2) | 0.131 |
| HDRS, mean (SD) | 1.13 (0.89) | 0.92 (0.70) | 0.17, −1.681 |
| HARS, mean (SD) | 23.35 (2.74) | 1.25 (1.01) | <0.001, −9.569 |
| PDSS, mean (SD) | 21.43 (1.91) | N/A | N/A |

Sig *P* (significance of *P* value) was from Mann–Whitney *U* test for nonparametric independent 2-sample *t* test.

F = female, *df* = degree of freedom, HARS = Hamilton Rating Scales for Anxiety, HDRS = Hamilton Rating Scales for Depression, M = male, N/A = not applicable, n = number, PDSS = panic disorder severity scale, SD = standard deviation.

TABLE 2. The Nodes and Edges Within the Significant Sub-network Differences Between Healthy Controls and Patients

| Node 1 | Node 2 | Edge | Test Statistic |
|---------|---------|--------------------|----------------|
| PHG.L | PreCG.L | PHG.L to PreCG.L. | 4.15 |
| PHG.L | DCG.L | PHG.L to DCG.L. | 4.49 |
| PHG.L | DCG.R | PHG.L to DCG.R. | 4.23 |
| PHG.L | SMG.L | PHG.L to SMG.L. | 4.68 |
| PHG.L | SMG.R | PHG.L to SMG.R. | 4.12 |
| PreCG.L | CAL.L | PreCG.L to CAL.L. | 4.41 |
| PreCG.L | CAL.R | PreCG.L to CAL.R. | 4.22 |
| PreCG.L | LING.R | PreCG.L to LING.R. | 4.37 |

CAL.L and CAL.R=left and right calcarine fissure, DCG.L and DCG.R=left and right middle cingulate gyrus, LING.R=right lingual gyrus, PHG.L=left parahippocampal gyrus, PreCG.L=left precentral gyrus, SMG.L and SMG.R=left and right supramarginal gyrus.

connectome of PDO. The edges between PHG, DCG, sensory, and motor regions also revealed the most top position of PHG in the functional connectome. At last, sensory regions, such as CAL, LING, and SMG, were also altered in PDO. The findings also suggested that further inclusion of sensory regions would make the original “fear network model” more comprehensive in understanding the sensory-related panic symptoms, such as chest tightness, lightheaded, and blurred vision. Our findings were also distinct from the findings of functional connectome alterations in another anxiety disorder, posttraumatic stress disorder, which showed significant alterations in default mode network and salience network.^{35,36}

Recently, the functional connectivity reports in PDO mostly focused on the seed-based approach by Rs-FMRI^{37–39} or region of interest approach by task-related FMRI.^{40–44} Most studies revealed the alteration of amygdala-based functional

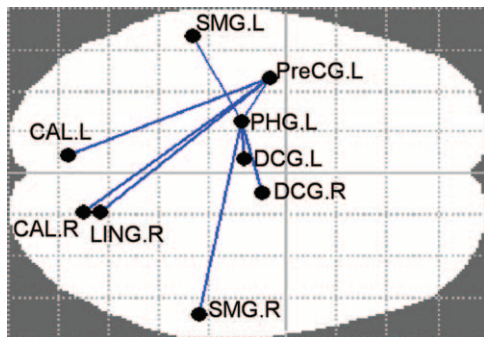


FIGURE 1. Alterations in the limbic-visuospatial network connectivity in PDO. Two central hubs were noted, which were PHG.L (limbic system) and PreCG.L (motor region). The sensory and visuospatial regions, such as CAL.L, CAL.R, SMG.L, SMG.R, and LING.R, were connected with the 2 central hubs. In addition, the 2 central hubs were connected, and the weakening edge between PHG.L and PreCG.L seemed to be modulated by PHG.L. Other limbic regions, DCG.L and DCG.R, were also connected with PHG.L in a weakening pattern. CAL.L and CAL.R=left and right calcarine fissure, DCG.L and DCG.R=left and right middle cingulate gyrus, LING.R=right lingual gyrus, PHG.L=left parahippocampal gyrus, PreCG.L=left precentral gyrus, SMG.L and SMG.R=left and right supramarginal gyrus.

connectivity. However, our study used the NBS methodology to avoid such seed-based or region-of-interest bias. Our results revealed the somatosensory network alterations in PDO, which were in line with the findings of a previous study.⁴⁵ According to our knowledge, this should be the first functional connectome study in PDO. The less-bias advantage of NBS method probably gives us a whole picture of functional connectome in PDO. A PHG-centered network with sensory and motor regions probably represented a revised version of “fear network” model for PDO.

The alterations of PHG has been mentioned in early articles of PDO, which included the elevation in cerebral blood flow, reductions in gray matter volume, and increased benzodiazepine receptor binding in PHG.^{5,8,9} However, the hypoperfusion results in PHG were reported in another study.⁴⁶ The inconsistent previous results suggested that PHG alterations might be inconclusive. In recent neuroimaging studies, our voxel-based morphometry study found that PDO comorbid with depression would have gray matter reductions in PHG.⁶ Our meta-analysis of gray matter studies also revealed that PHG has been a common pathology for PDO.⁷ Two antidepressant studies in PDO also demonstrated that antidepressant treatment would increase glucose metabolism in cerebral cortex and limbic regions, which also included the PHG.L and PreCG.L.^{47,48} However, recent functional connectivity study in PDO revealed no significant finding in PHG. Our results in PHG.L and its central hub role in current analysis of functional connectome probably represented a large-scale neurophysiological alteration in PDO. The altered connectivity between PHG and DCG probably suggested that altered intralimbic edge would also influence origin of PDO. The results were also in line with the lower activities of DCG⁴⁹ and treatment response-related influences of neuronal stability in DCG⁵⁰ in PDO.

The PreCG, a motor region, has been ignored in the pathophysiology of PDO for a long duration. However, several early studies mentioned the activity changes in PreCG after panic-provoking challenges,⁹ increasing activities after stimulus of spatial unpredictability⁵¹ and increasing activities during anxiety status.⁵² Our previous study in PDO revealed residual gray matter deficits in PreCG even after remission under antidepressant treatment.⁵³ Another study also indicated that cognitive behavioral therapy would be associated with increased regional cerebral blood flow in PreCG.⁵⁴ In addition, the gray matter reductions in PreCG seemed to be a shared pathophysiology of anxiety.^{55,56} The Rs-FMRI study also supported the role of PreCG in neuronal stability and synchronization of anxiety.⁵⁷ Functional connectivity survey showed inconsistent results, from negative results in anxiety disorders⁵⁸ to altered connectivity between PreCG and frontal lobe in posttraumatic stress disorder.⁵⁹ In the current study, PreCG play second central hub for altered functional connectivity network in PDO. The results suggested the motor response of PDO probably would have negative feedback for sensory reception of panic-provoking stimulus. However, more studies are warranted to clarify the causality of PreCG-related functional connectivity.

The sensory regions, such as CAL, LING, and SMG, seemed to be under the influences of PHG and PreCG. The hyperperfusion of cerebral blood flow in SMG and temporal lobe has been reported in PDO.⁴⁶ In addition, the activities in SMG and temporal lobe were also associated with the severity of psychopathology in PDO.⁶⁰ The decreased connectivity strength between PHG.L and SMG also corresponded to the altered activities in temporal lobe and SMG in PDO. The study

of neutral face task found decreased activities in CAL and other visual areas of PDO patients.⁶¹ CAL, an area of visuosensory function, was the terminus of nervous impulses generated in the retina and where simple visual sensations arose.⁶² The processing of emotional faces was also associated with hypoactivation in the LING of PDO patients.⁴⁰ However, Pannekoeck et al⁵⁸ found no significant alterations in functional connectivity between LING, CAL, and PreCG in any anxiety disorder. The spatial scene memory and allocentric coding might be disturbed in PDO.⁶³ The weakening connectivity of PreCG-CAL and PreCG-LING probably suggested the weakening feedback and control ability for these sensory regions, which would provoke panic attacks under oversensitivity status. Further study would be needed to clarify the complex relationship between limbic, motor, and sensory regions.

Limitations

There were several limitations in the current study. First, the cross-sectional design would limit the interpretations of our study results. A future longitudinal study would help us confirm the importance of “limbic-motor-sensory” network in PDO. A possible selection bias due to the overlap of current study sample with our previous study sample would also influence our results. Second, this study just provided the functional connectome results without the ground for structural connectome data. The future NBS analysis with structural imaging data derived from as T1 gray matter imaging and diffusion tensor imaging would help illuminate the structural connectome ground for functional connectome results. Third, functional connectome measures the functional connectivity according to the signals of hemodynamics. The alterations of functional connectome are probably related to the hemodynamic changes. However, it is still unknown whether the method of functional connectome can be used to detect early neuronal changes, or monitor disease progression in PDO. Fourth, a task-oriented functional MRI study could complete the viewpoint due to Rs-fMRI characteristics of the functional connectome results. Fifth, the lack of visuospatial data in current sample might limit the interpretation of “limbic-motor-sensory” revision in “fear network” model for PDO.

CONCLUSIONS

The analysis of functional connectome revealed a pattern of “limbic-motor-sensory” connectivity alteration in PDO. A revision of fear network model can probably be considered under the impression of current study results.

ACKNOWLEDGMENTS

The authors acknowledge the grant support from Taipei Tzu-Chi General Hospital Project, Cheng Hsin General Hospital, and National Yang Ming University Cooperative Project 105F003C03. The authors also acknowledge MR support from National Yang-Ming University, Taiwan, which is in part supported by the MOE plan for the top university.

REFERENCES

- Weissman MM, Wickramaratne P, Adams PB, et al. The relationship between panic disorder and major depression. A new family study. *Arch Gen Psychiatry*. 1993;50:767–780.
- Culpepper L. Identifying and treating panic disorder in primary care. *J Clin Psychiatry*. 2004;65(Suppl 5):19–23.
- Gorman JM, Kent JM, Sullivan GM, et al. Neuroanatomical hypothesis of panic disorder, revised. *Am J Psychiatry*. 2000;157:493–505.
- Dresler T, Guhn A, Tupak SV, et al. Revise the revised? New dimensions of the neuroanatomical hypothesis of panic disorder. *J Neural Transm*. 2013;120:3–29.
- Massana G, Serra-Grabulosa JM, Salgado-Pineda P, et al. Parahippocampal gray matter density in panic disorder: a voxel-based morphometric study. *Am J Psychiatry*. 2003;160:566–568.
- Lai CH, Hsu YY, Wu YT. First episode drug-naïve major depressive disorder with panic disorder: gray matter deficits in limbic and default network structures. *Eur Neuropsychopharmacol*. 2010;20:676–682.
- Lai CH. Gray matter deficits in panic disorder: a pilot study of meta-analysis. *J Clin Psychopharmacol*. 2011;31:287–293.
- Hasler G, Nugent AC, Carlson PJ, et al. Altered cerebral gamma-aminobutyric acid type A-benzodiazepine receptor binding in panic disorder determined by [¹¹C]flumazenil positron emission tomography. *Arch Gen Psychiatry*. 2008;65:1166–1175.
- Boshuisen ML, Ter Horst GJ, Paans AM, et al. rCBF differences between panic disorder patients and control subjects during anticipatory anxiety and rest. *Biol Psychiatry*. 2002;52:126–135.
- Uchida RR, Del-Ben CM, Busatto GF, et al. Regional gray matter abnormalities in panic disorder: a voxel-based morphometry study. *Psychiatry Res*. 2008;163:21–29.
- Jackson PL, Meltzoff AN, Decety J. Neural circuits involved in imitation and perspective-taking. *Neuroimage*. 2006;31:429–439.
- Kitada R, Johnsrude IS, Kochiyama T, et al. Brain networks involved in haptic and visual identification of facial expressions of emotion: an fMRI study. *Neuroimage*. 2010;49:1677–1689.
- Taylor SF, Liberzon I, Fig LM, et al. The effect of emotional content on visual recognition memory: a PET activation study. *Neuroimage*. 1998;8:188–197.
- Gundel H, O'Connor MF, Littrell L, et al. Functional neuroanatomy of grief: an fMRI study. *Am J Psychiatry*. 2003;160:1946–1953.
- Spoormaker VI, Sturm A, Andrade KC, et al. The neural correlates and temporal sequence of the relationship between shock exposure, disturbed sleep and impaired consolidation of fear extinction. *J Psychiatr Res*. 2010;44:1121–1128.
- Carlson JM, Reinke KS, Habib R. A left amygdala mediated network for rapid orienting to masked fearful faces. *Neuropsychologia*. 2009;47:1386–1389.
- Zalesky A, Fornito A, Bullmore ET. Network-based statistic: identifying differences in brain networks. *Neuroimage*. 2010;53:1197–1207.
- Korgaonkar MS, Fornito A, Williams LM, et al. Abnormal structural networks characterize major depressive disorder: a connectome analysis. *Biol Psychiatry*. 2014;76:567–574.
- Long Z, Duan X, Wang Y, et al. Disrupted structural connectivity network in treatment-naïve depression. *Prog Neuropsychopharmacol Biol Psychiatry*. 2015;56:18–26.
- Lako IM, Wigman JT, Klaassen RM, et al. Psychometric properties of the self-report version of the Quick Inventory of Depressive Symptoms (QIDS-SR(1)(6)) questionnaire in patients with schizophrenia. *BMC Psychiatry*. 2014;14:247. doi:10.1186/s12888-014-0247-2.
- Nasr SJ, Altman EG, Rodin MB, et al. Correlation of the Hamilton and Carroll Depression Rating Scales: a replication study among psychiatric outpatients. *J Clin Psychiatry*. 1984;45:167–168.
- Sugarman MA, Loree AM, Baltes BB, et al. The efficacy of paroxetine and placebo in treating anxiety and depression: a meta-

- analysis of change on the Hamilton Rating Scales. *PLoS One*. 2014;9:e106337.
23. Argyle N, Deltito J, Allerup P, et al. The Panic-Associated Symptom Scale: measuring the severity of panic disorder. *Acta Psychiatr Scand*. 1991;83:20–26.
 24. Lai CH, Wu YT. The alterations in inter-hemispheric functional coordination of patients with panic disorder: The findings in the posterior sub-network of default mode network. *J Affect Disord*. 2014;166:279–284.
 25. Oldfield RC. The assessment and analysis of handedness: the Edinburgh inventory. *Neuropsychologia*. 1971;9:97–113.
 26. Lai CH, Wu YT. Fronto-occipital fasciculus, corpus callosum and superior longitudinal fasciculus tract alterations of first-episode, medication-naïve and late-onset panic disorder patients. *J Affect Disord*. 2013;146:378–382.
 27. Lai CH, Wu YT. Alterations in white matter micro-integrity of the superior longitudinal fasciculus and anterior thalamic radiation of young adult patients with depression. *Psychol Med*. 2014;44:2825–2832.
 28. Chao-Gan Y, Yu-Feng Z. DPARSF: A MATLAB toolbox for “pipeline” data analysis of resting-state fMRI. *Front Syst Neurosci*. 2010;4:13. doi: 10.3389/fnsys.2010.00013.
 29. Yan CG, Cheung B, Kelly C, et al. A comprehensive assessment of regional variation in the impact of head micromovements on functional connectomics. *Neuroimage*. 2013;76:183–201.
 30. Power JD, Barnes KA, Snyder AZ, et al. Spurious but systematic correlations in functional connectivity MRI networks arise from subject motion. *Neuroimage*. 2012;59:2142–2154.
 31. Fox MD, Snyder AZ, Vincent JL, et al. The human brain is intrinsically organized into dynamic, anticorrelated functional networks. *Proc Natl Acad Sci U S A*. 2005;102:9673–9678.
 32. Murphy K, Birn RM, Handwerker DA, et al. The impact of global signal regression on resting state correlations: are anti-correlated networks introduced? *Neuroimage*. 2009;44:893–905.
 33. Yan CG, Craddock RC, He Y, et al. Addressing head motion dependencies for small-world topologies in functional connectomics. *Front Hum Neurosci*. 2013;7:910.
 34. Dresler T, Guhn A, Tupak SV, et al. Revise the revised? New dimensions of the neuroanatomical hypothesis of panic disorder. *J Neural Transm (Vienna)*. 2013;120:3–29.
 35. Lei D, Li K, Li L, et al. Disrupted functional brain connectome in patients with posttraumatic stress disorder. *Radiology*. 2015;276:818–827.
 36. Jin C, Qi R, Yin Y, et al. Abnormalities in whole-brain functional connectivity observed in treatment-naïve post-traumatic stress disorder patients following an earthquake. *Psychol Med*. 2014;44:1927–1936.
 37. Hahn A, Stein P, Windischberger C, et al. Reduced resting-state functional connectivity between amygdala and orbitofrontal cortex in social anxiety disorder. *Neuroimage*. 2011;56:881–889.
 38. Pannekoek JN, Veer IM, van Tol MJ, et al. Aberrant limbic and salience network resting-state functional connectivity in panic disorder without comorbidity. *J Affect Disord*. 2013;145:29–35.
 39. Shin YW, Dzemidzic M, Jo HJ, et al. Increased resting-state functional connectivity between the anterior cingulate cortex and the precuneus in panic disorder: resting-state connectivity in panic disorder. *J Affect Disord*. 2013;150:1091–1095.
 40. Demenescu LR, Kortekaas R, Cremers HR, et al. Amygdala activation and its functional connectivity during perception of emotional faces in social phobia and panic disorder. *J Psychiatr Res*. 2013;47:1024–1031.
 41. Kircher T, Arolt V, Jansen A, et al. Effect of cognitive-behavioral therapy on neural correlates of fear conditioning in panic disorder. *Biol Psychiatry*. 2013;73:93–101.
 42. Leicht G, Mulert C, Eser D, et al. Benzodiazepines counteract rostral anterior cingulate cortex activation induced by cholecystokinin-tetrapeptide in humans. *Biol Psychiatry*. 2013;73:337–344.
 43. Straube B, Lueken U, Jansen A, et al. Neural correlates of procedural variants in cognitive-behavioral therapy: a randomized, controlled multicenter fMRI study. *Psychother Psychosom*. 2014;83:222–233.
 44. Lueken U, Straube B, Wittchen HU, et al. Therapygenetics: anterior cingulate cortex-amygdala coupling is associated with 5-HTTLPR and treatment response in panic disorder with agoraphobia. *J Neural Transm*. 2015;122:135–144.
 45. Peterson A, Thome J, Frewen P, et al. Resting-state neuroimaging studies: a new way of identifying differences and similarities among the anxiety disorders? *Can J Psychiatry*. 2014;59:294–300.
 46. Koh KB, Kang JI, Lee JD, et al. Shared neural activity in panic disorder and undifferentiated somatoform disorder compared with healthy controls. *J Clin Psychiatry*. 2010;71:1576–1581.
 47. Sim HB, Kang EH, Yu BH. Changes in cerebral cortex and limbic brain functions after short-term paroxetine treatment in panic disorder: an [F]FDG-PET pilot study. *Psychiatry Investig*. 2010;7:215–219.
 48. Kang EH, Park JE, Lee KH, et al. Regional brain metabolism and treatment response in panic disorder patients: an [18F]FDG-PET study. *Neuropsychobiology*. 2012;66:106–111.
 49. Moon CM, Yang JC, Jeong GW. Explicit verbal memory impairments associated with brain functional deficits and morphological alterations in patients with generalized anxiety disorder. *J Affect Disord*. 2015;186:328–336.
 50. Lai CH, Wu YT. The changes in the low-frequency fluctuations of cingulate cortex and postcentral gyrus in the treatment of panic disorder: The MRI study. *World J Biol Psychiatry*. 2015;1–8.
 51. Hahn B, Ross TJ, Stein EA. Neuroanatomical dissociation between bottom-up and top-down processes of visuospatial selective attention. *Neuroimage*. 2006;32:842–853.
 52. Kilts CD, Kelsey JE, Knight B, et al. The neural correlates of social anxiety disorder and response to pharmacotherapy. *Neuropsychopharmacology*. 2006;31:2243–2253.
 53. Lai CH, Wu YT. Changes in gray matter volume of remitted first-episode, drug-naïve, panic disorder patients after 6-week antidepressant therapy. *J Psychiatr Res*. 2013;47:122–127.
 54. Seo HJ, Choi YH, Chung YA, et al. Changes in cerebral blood flow after cognitive behavior therapy in patients with panic disorder: a SPECT study. *Neuropsychiatr Dis Treat*. 2014;10:661–669.
 55. Shang J, Fu Y, Ren Z, et al. The common traits of the ACC and PFC in anxiety disorders in the DSM-5: meta-analysis of voxel-based morphometry studies. *PLoS One*. 2014;9:e93432.
 56. Strawn JR, Wehry AM, Chu WJ, et al. Neuroanatomic abnormalities in adolescents with generalized anxiety disorder: a voxel-based morphometry study. *Depress Anxiety*. 2013;30:842–848.
 57. Zhang Y, Zhu C, Chen H, et al. Frequency-dependent alterations in the amplitude of low-frequency fluctuations in social anxiety disorder. *J Affect Disord*. 2015;174:329–335.
 58. Pannekoek JN, van der Werff SJ, van Tol MJ, et al. Investigating distinct and common abnormalities of resting-state functional connectivity in depression, anxiety, and their comorbid states. *Eur Neuropsychopharmacol*. 2015;25:1933–1942.
 59. Kennis M, Rademaker AR, van Rooij SJ, et al. Resting state functional connectivity of the anterior cingulate cortex in veterans

- with and without post-traumatic stress disorder. *Hum Brain Mapp.* 2015;36:99–109.
60. Wintermann GB, Donix M, Joraschky P, et al. Altered olfactory processing of stress-related body odors and artificial odors in patients with panic disorder. *PLoS One.* 2013;8:e74655.
61. Petrowski K, Wintermann G, Smolka MN, et al. The neural representation of emotionally neutral faces and places in patients with panic disorder with agoraphobia. *J Affect Disord.* 2014;152–154454-61.
62. Macmillan M. Alfred Walter Campbell and the visual functions of the occipital cortex. *Cortex.* 2014;56:157–181.
63. Schmidt D, Krause BJ, Weiss PH, et al. Visuospatial working memory and changes of the point of view in 3D space. *Neuroimage.* 2007;36:955–968.